

INELASTIC BUCKLING PROCESS OF AXIALLY COMPRESSED CYLINDRICAL SHELLS SUBJECT TO EDGE CONSTRAINTS

L. M. MURPHY†

Analytical Mechanics Division 8352, Sandia Corporation, Livermore, California 94550

and

L. H. N. LEE‡

University of Notre Dame, Notre Dame, Indiana 46556

Abstract—In this paper the effects of prebuckling deformation caused by edge constraints, and non linear strain displacement relationships, on the inelastic buckling process of axially compressed cylindrical shells are studied. By Drucker's postulate of positive work in plastic deformation, a modified incremental theory of plasticity on the stress-strain relationships expressed in terms of Kirchhoff stress and Green strain rates is developed. A variational principle in the Lagrangian description and for quasi-static problems of finite plasticity is developed, and the existence of an extremum principle for a material having a sufficiently great hardening rate is shown. In addition a criterion for the stability of a body under dead load is established.

The variational principle in conjunction with the incremental Rayleigh-Ritz technique is used to determine the deformation process of an idealized cylindrical shell composed of four thin load carrying sheets made of a general work hardening material. The theoretical predictions obtained numerically by digital computer compare favorably with available experimental results.

INTRODUCTION

THE cylindrical shell has been one of the most commonly used elements in modern structures, and has stimulated considerable interest in the theory of thin shells. A major problem of interest is to determine the inelastic buckling process of the axially compressed cylindrical shells [1-7]. Existing solutions are based on the small deflection assumption, the stress-strain relationships by either the incremental [8, 9] or deformation [10] theories of plasticity, uniform material response and idealized boundary conditions. In this paper these assumptions and conditions are re-evaluated.

In most existing analyses, the critical load at which a bifurcation of stable equilibrium configurations of an axially compressed cylindrical shell is determined. It is found that the critical axial loads based on the deformation theory, which assumes a one to one correspondence between stress and strain and ignores the material stress history, often agree quite well with experimental maximum loads. For the relatively more rigorous incremental theory, this is not the case.

It is implied in most existing analyses that a cylinder just prior to buckling, in the sense of bifurcation, is perfectly cylindrical and is in a state of uniform axial stress. It is further assumed that axial loading and bending occur simultaneously such that no strain reversal

† Technical Staff Member.

‡ Professor of Aerospace and Mechanical Engineering.

takes place. In reality, edge constraints produce bending waves, thus the assumption of a simple stress state and hence uniform material response may not be realistic near the buckling load, as demonstrated by Lee [11] in a recent paper. In considering the effects of prebuckling deformation and edge constraints, Lee determined the critical load of unloading corresponding to axisymmetric deformation. The presence of non-uniform prebuckling deformation indicates the possibility of a continuous and complex deformation process rather than an abrupt geometrical change as implied by the bifurcation analyses. By investigating this total buckling process rather than a single characteristic or critical load, additional insight may be added to the instability process.

In this paper, the inelastic buckling process of an axially compressed circular cylindrical shell with edge constraints is studied by an approach using the relatively rigorous incremental theory of plasticity which considers the material stress history. Furthermore, the effects of the nonlinear strain-displacement relationships, initial imperfections and edge constraints on the prebuckling and postbuckling process are analyzed. A variational procedure for quasi-static problems of finite plasticity [24] is used to determine the effect of these considerations. The variational principle is derived from a set of rate equilibrium equations.

A numerical procedure based on an incremental Rayleigh-Ritz technique is employed to determine the velocity field for a prescribed loading rate and the subsequent deformation process including the maximum load. To make the amount of computation tenable, an idealized sandwich shell, having four thin adjacent load-carrying sheets made of a general work hardening material, is employed. The numerically determined maximum loads are compared with available results.

THE VARIATIONAL PRINCIPLE

For treating quasi-static problems of inelasticity, variational principles expressed in terms of stress and strain rates, and velocity fields have been suggested [12-15]. The following variational principle for quasi-static problems of finite plasticity is formulated in a similar spirit.

Consider a body of continuum occupying a region V bounded by a surface $S = S_u + S_T$ in the current (deformed) state, which corresponds to a region V_0 with a boundary surface $S_0 = S_{0u} + S_{0T}$ in the natural (undeformed) state. Let the initial position of a particle in the body be at a_i in a three dimensional space and its current (displaced) position be at X_i in the same space. Let u_i be the displacement vector of the particle, i.e. $u_i = X_i - a_i$. The body is subjected to a body force per unit mass F_i , a surface traction T_i over the portion of the boundary surface S_T and specified displacement u_i over the portion of the boundary surface S_u . The following relationships may be defined:

$$\begin{aligned} \rho_0 dV_0 &= \rho dV \\ F_{0,i} \rho_0 dV_0 &= F_i \rho dV \end{aligned} \quad (1)$$

and

$$T_{0,i} dS_0 = T_i dS$$

where ρ_0 is the natural mass density which corresponds to the density ρ in the current state. $F_{0,i}$ and $T_{0,i}$ are the conceptual body force and surface traction associated with the

natural state. For convenience in expressing a stress-strain law, the symmetric Kirchhoff stress tensor, S_{ij} , may be used [16]. The Kirchhoff stress tensor is defined by its relationship with the Eulerian (true) stress tensor σ_{ij} , or

$$S_{ij} = \frac{\rho_0}{\rho} \frac{\partial a_i}{\partial X_\eta} \frac{\partial a_j}{\partial X_\xi} \sigma_{\eta\xi}. \tag{2}$$

By its definition, the Kirchhoff stress tensor has the following relationship with the surface traction

$$n_{0i} S_{ij} X_{k,j} = T_{0k} \text{ over } S_{0r} \tag{3}$$

where an index j following a comma indicates partial differentiation with respect to a_j and the repetition of an index in a term denotes a summation with respect to that index over its range. n_{0i} is the unit outer normal vector of the original surface area dS_0 . It may be shown that the equilibrium of any portion of the body requires that

$$[S_{jk}(\delta_{ik} + u_{i,k})]_{,j} + \rho_0 F_{0i} = 0 \tag{4}$$

where δ_{ik} is the Kronecker delta. Differentiating equation (4) with respect to time, we find

$$\left\{ \frac{\partial}{\partial t} [S_{jk}(\delta_{ik} + u_{i,k})] \right\}_{,j} + \rho_0 \dot{F}_{0i} = 0. \tag{5}$$

Consider a class of arbitrary virtual velocities $\delta \dot{u}_i$ which are continuous, triply differentiable over the domain V_0 , and which vanish over the boundary surface S_{0u} , whereon values of velocities are prescribed. Multiplying equation (5) by $\delta \dot{u}_i$ and integrating the products over V_0 , it is found that

$$\int_{V_0} \left\{ \frac{\partial}{\partial t} [S_{jk}(\delta_{ik} + u_{i,k})] \right\}_{,j} \delta \dot{u}_i dV_0 + \int_{V_0} \rho_0 \dot{F}_{0i} \delta \dot{u}_i dV_0 = 0. \tag{6}$$

On introducing

$$n_{0j} \frac{\partial}{\partial t} [S_{jk}(\delta_{ik} + u_{i,k})] = \dot{T}_{0i}$$

and using Gauss theorem, we obtain the variational equation of equilibrium

$$\int_{V_0} \dot{S}_{ij} \delta \dot{\epsilon}_{ij} dV_0 + \int_{V_0} S_{ij} \dot{u}_{k,i} \delta \dot{u}_{k,j} dV_0 = \int_{V_0} \rho_0 \dot{F}_{0i} \delta \dot{u}_i dV_0 + \int_{S_0} \dot{T}_{0i} \delta \dot{u}_i dS_0 \tag{7}$$

where ϵ_{ij} is the Green strain tensor [14] or

$$\epsilon_{ij} = \frac{1}{2}(u_{i,j} + u_{j,i} + u_{k,i} u_{k,j}) \tag{8}$$

and

$$\delta \dot{\epsilon}_{ij} = \frac{1}{2}(\delta \dot{u}_{i,j} + \delta \dot{u}_{j,i} + \delta \dot{u}_{k,i} u_{k,j} + u_{k,i} \delta \dot{u}_{k,j}). \tag{9}$$

Equation (7) may be put into a more familiar form by introducing a strain rate potential obtained by the following consideration on the stress-strain relationship.

From a continuum view point, there are two popular types of constitutive relations in plasticity, incremental theories and deformation or total strain theories [17]. The deformation theories postulate a unique relation between stress and total strain. In general,

this is physically unacceptable because plastic deformation is path dependent and irreversible. However, for some simple loading paths, the deformation theories may be considered as a mathematical approximation [10].

The isothermal incremental theories are based on Drucker's fundamental postulate [8] which may be stated as follows: consider an element initially in some state of stress, to which by an external agency an additional set of stresses is slowly applied and slowly removed. Then the work done by the external agency is positive during the process. In his evaluation of infinitesimal plastic deformation, Drucker employed the Eulerian stress tensor and deformation rate tensor, $\dot{\epsilon}_{ij}$, in describing the rate of doing work, DW/Dt , per unit mass, or

$$\frac{DW}{Dt} = \frac{1}{\rho} \sigma_{ij} \dot{\epsilon}_{ij}. \tag{10}$$

It may be shown that, in terms of the Lagrangian variables, the rate of doing work may be written as

$$\frac{DW}{Dt} = \frac{1}{\rho} S_{ij} \dot{\epsilon}_{ij}. \tag{11}$$

Assuming the existence of a loading surface [$f(S_{ij}) = C$] in the stress space, Drucker's postulate and equation (11) establish two requirements: (a) the loading surface is convex and (b) at a smooth point of $f = C$, the plastic strain rate vector is always directed along the normal to the loading surface. In other words, the isothermal relationships between Kirchhoff stress rates and Green strain rates may be written as

$$\dot{\epsilon}_{ij} = \dot{\epsilon}_{ij}^e + \dot{\epsilon}_{ij}^p = \left(C_{ijkl} + G \frac{\partial f}{\partial S_{kl}} \right) \dot{S}_{kl} \quad \text{for } f = C \text{ and } df > 0$$

or

$$\dot{\epsilon}_{ij} = \dot{\epsilon}_{ij}^e = C_{ijkl} \dot{S}_{kl} \quad \text{for } f < C \text{ or } df \leq 0$$

where $\dot{\epsilon}_{ij}^e$ is the elastic strain-rate and G and f are functions of the state of the material, which may include the strain and the history of loading as well as the existing state of stress. The coefficients C_{ijkl} may be functions of the existing state of stress or constants.

A loading function for finite plasticity, f , expressed in terms of Kirchhoff stresses has been employed by Green and Naghdi [18]. The constitutive relationships given by equation (12) do satisfy the coordinate and spatial invariance and thermodynamics requirements under isothermal conditions.

The inversions of equation (12) may be written as

$$\dot{S}_{ij} = \bar{C}_{ijkl} \dot{\epsilon}_{kl} \quad \text{for } f < C \text{ or } df \leq 0$$

or

$$\dot{S}_{ij} = \bar{D}_{ijkl} \dot{\epsilon}_{kl} \quad \text{for } f = C \text{ and } df > 0.$$

Analogous to the elastic strain-energy function, the strain-rate potential

$$U(\dot{\epsilon}_{ij}) = \bar{C}_{ijkl} \dot{\epsilon}_{ij} \dot{\epsilon}_{kl} \quad \text{for } f < C \text{ or } df \leq 0$$

or

$$U(\dot{\epsilon}_{kj}) = \bar{D}_{ijkl}\dot{\epsilon}_{ij}\dot{\epsilon}_{kl} \quad \text{for } f = C \text{ and } df > 0 \tag{14}$$

may be established such that

$$\frac{\partial U}{\partial \dot{\epsilon}_{ij}} = \dot{S}_{ij} \quad \text{and} \quad \delta U = \dot{S}_{ij}\delta\dot{\epsilon}_{ij}. \tag{15}$$

Substituting equation (14) into (7), it is found that

$$\delta[I(\dot{u}_i)] = \delta \left[\int_{V_0} (U + \frac{1}{2}S_{ij}\dot{u}_{k,i}\dot{u}_{k,j}) dV_0 - \int_{V_0} \rho_0 \dot{F}_0 \dot{u}_i dV_0 - \int_{S_0} \dot{T}_0 \dot{u}_i dS_0 \right] = 0. \tag{16}$$

In carrying out the integral in equation (16), the regions of loading ($df > 0$) and unloading ($df \leq 0$) required in formulating the strain-rate potential U are assumed. In carrying out the variational process the stress-rate variations are only allowed along some permissible paths [15] from state 1 to state 2 such that

$$[(\dot{S}_{ij})_2 - (\dot{S}_{ij})_1][(\dot{\epsilon}_{ij})_2 - (\dot{\epsilon}_{ij})_1] > 0. \tag{17}$$

Furthermore, the assumed regions of loading and unloading must agree with the determined regions of loading and unloading. In the direct method of calculation, this may be accomplished by a trial and error process, if the trend of deformation is followed.

By comparing the value of the functional $I(\dot{u}_i)$ in equation (16) for any distinct compatible velocity field, \dot{u}'_i , with that for the true velocity field, \dot{u}^*_i , it may be shown that the functional has an absolute minimum value for the true velocity field when the following inequality is satisfied :

$$I(\dot{u}'_i) - I(\dot{u}^*_i) = \frac{1}{2} \int_{V_0} \Delta \dot{S}_{ij} \Delta \dot{\epsilon}_{ij} dV_0 + \frac{1}{2} \int_{V_0} S_{ij} \Delta \dot{u}_{k,i} \Delta \dot{u}_{k,j} dV_0 > 0 \tag{18}$$

where $\Delta \dot{u}_i = \dot{u}'_i - \dot{u}^*_i$.

The integral

$$\frac{1}{2} \int_{V_0} \Delta \dot{S}_{ij} \Delta \dot{\epsilon}_{ij} dV_0$$

is positive if the variations are only allowed along permissible paths specified by inequality (17). The value of the integral depends on the rates of hardening or the values of \bar{C}_{ijkl} and \bar{D}_{ijkl} in equation (13). The other integral in equation (18) may or may not be positive depending on the current state of stress and deformation. Therefore, the extremum property and the implied uniqueness of the solution of the problem exists only for sufficiently great rates of hardening.

It is of interest to note that the criterion (18) for the extremum property is related to a criterion for the stability of an equilibrium state in the following sense. The classical definition of stability by Dirichlet and Kelvin may be stated as follows. A body is in a state of stable equilibrium if, in the motion following any kind of transitory disturbance, the amplitude of the additional displacement is always vanishingly small when the disturbance itself is vanishingly small. According to this definition, a sufficient condition for stability is that in any possible infinitesimal displacement from the position of equilibrium, the internal energy stored or dissipated should exceed the work done on the system by

the acting external forces. This permits the containment or decay of the kinetic energy caused by the external disturbance. Consider an arbitrary, compatible displacement, Δu_i , which occurs fictitiously in the time interval Δt . The above condition leads to

$$\int_{V_0} \left[\int_{t_0}^{t_0+\Delta t} S_{ij} \dot{\epsilon}_{ij} dt \right] dV_0 - \int_{S_0} \left[T_{0,i}^0 \int_{t_0}^{t_0+\Delta t} \dot{u}_i dt \right] dS_0 - \int_{V_0} \left[F_{0,i}^0 \rho_0 \int_{t_0}^{t_0+\Delta t} \dot{u}_i dt \right] dV_0 = \int \left[\frac{1}{2} \Delta S_{ij} \Delta \epsilon_{ij} + \frac{1}{2} S_{ij}^0 \Delta u_{k,i} \Delta u_{k,j} \right] dV_0 > 0 \tag{19}$$

where superscript 0 of a quantity denotes the quantity at t_0 . The inequality (19) remains valid when both sides are divided by Δt^2 and may be expressed as

$$\int_{V_0} (\dot{S}_{ij} \dot{\epsilon}_{ij} + S_{ij}^0 \dot{u}_{k,i} \dot{u}_{k,j}) dV_0 > 0. \tag{20}$$

Inequalities (18) and (20) appear to be similar and yet they are distinct criteria. Criterion (18) is for any pair of velocity fields satisfying the constraints whereas criterion (20) is for any velocity field satisfying the constraints therefore, the inequality (20) is always satisfied when inequality (18) is (but not vice versa); for (18) reduces to (20) when one field of a pair is null. Therefore, it is possible that, at a certain state, the solution of the incremental boundary value problem is not unique yet the state may be stable. An example is the bifurcation phenomenon at the tangent modulus load of an inelastic column as illustrated by Shanley [19, 20]. It is to be noted that, whether the solution is unique or not, the variational principle by equation (16) remains valid for an equilibrium solution.

The foregoing uniqueness and stability criteria are essentially identical to that obtained by Hill [14] except that they differ in form. Hill expresses his results in terms of Lagrangian or "nominal" stress rate tensor which is not symmetrical and has a comparatively involved constitutive relationship with the velocity gradient. The results in this paper are expressed in terms of the Kirchhoff stress rate tensor which is symmetric and has relatively a simple constitutive relationship with the Green strain rate tensor.

SHELL GEOMETRY

Consider a simply supported cylindrical shell of uniform thickness h and length $2L$, with or without geometrical imperfections as shown in Fig. 1. Let \bar{x} , \bar{z} and θ denote the axial, radial and circumferential coordinates of the undeformed middle surface of radius R , as shown in Fig. 1. The radial difference between the radial distance of a point at the middle surface and the mean radius is denoted by

$$\bar{w}_{tot} = \bar{w} + \hat{w} \tag{21}$$

where \bar{w} and \hat{w} (both positive inward) are respectively, the displacement due to loading and the initial imperfection. The axial and circumferential displacement of a point on the middle surface of the shell is denoted by \bar{u} and \bar{v} respectively.

The following assumptions usually considered in the theories of thin shells are made:

- (a) The displacements are small in comparison to the length or radius of the cylinder, but may be of magnitude comparable to the thickness; and

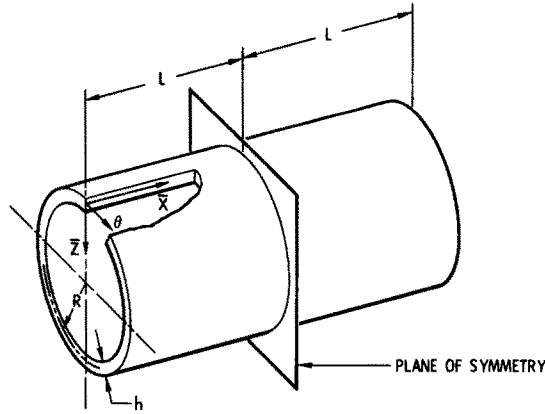


FIG. 1. Shell geometry.

(b) normal stresses in the radial direction are negligible and lines originally normal to the middle surface of the shell remain so after deformation.

To simplify the subsequent analysis, the following non-dimensional quantities are introduced

$$x = \frac{\bar{x}}{R}, \quad z = \frac{\bar{z}}{R}, \quad u = \frac{\bar{u}}{R}, \quad v = \frac{\bar{v}}{R}, \quad w = \frac{\bar{w}}{R} \tag{22}$$

and

$$\hat{w} = \frac{\hat{\bar{w}}}{R}.$$

The normal and shear strains may be shown to be

$$\begin{aligned} \epsilon_x &= u_{,x} + \frac{1}{2}w_{,x}^2 + \hat{w}_{,x}w_{,x} - zw_{,xx} \\ \epsilon_\theta &= v_{,\theta} - w + \frac{1}{2}w_{,\theta}^2 + w_{,\theta}\hat{w}_{,\theta} - z(w_{,\theta\theta} + v_{,\theta}) \\ \gamma_{x\theta} &= u_{,\theta} + v_{,x}(1-z) + w_{,\theta}w_{,x} + w_{,\theta}\hat{w}_{,x} + w_{,\theta}\hat{w}_{,x} - 2zw_{,x\theta}. \end{aligned} \tag{23}$$

Since both ends of the shell are hinged, the deformation will be symmetrical with respect to the plane at $x = L/R$. The boundary conditions for the hinged end are

$$v = w = w_{,xx} = 0 \quad \text{at } x = 0 \tag{24}$$

and the boundary conditions at the plane of symmetry are

$$u = v_{,x} = w_{,x} = 0 \quad \text{at } x = L/R. \tag{25}$$

Further simplification of the axial strain may be made by letting

$$u = u_B + u_S \tag{26}$$

and

$$u_B = \int_x^{L/R} (\frac{1}{2}w_{,x}^2 + w_{,x}\hat{w}_{,x}) dx \tag{27}$$

where both u_B and u_S are zero at $x = L/R$.

The quantity u_B may be interpreted as that part of the axial deformation of the middle surface associated with the inextensible bending of the middle surface. Then the axial strain may be shown to be

$$\varepsilon_x = u_{S,x} - z w_{,xx}. \quad (28)$$

In the subsequent analysis, the strain and displacement rates or increments are used in addition to the total radial displacement. The pertinent quantities are presented here for completeness.

$$\begin{aligned} \dot{\varepsilon}_x &= \dot{u}_{S,x} - z \dot{w}_{,xx} \\ \dot{\varepsilon}_\theta &= \dot{v}_\theta - \dot{w} + H_\theta \dot{w}_{,\theta} - z(\dot{w}_{,\theta\theta} + \dot{v}_{,\theta}) \\ \dot{\gamma}_{x\theta} &= \dot{u}_{S,\theta} + \dot{v}_{,x}(1-z) + H_x \dot{w}_{,\theta} + H_\theta \dot{w}_{,x} - 2z w_{,x\theta} \\ \dot{u}_B &= \int_x^{L/R} H_x \dot{w}_{,x} dx \end{aligned} \quad (29)$$

where

$$\begin{aligned} H_x &= w_{,x} + \hat{w}_{,x} \\ H_\theta &= w_{,\theta} + \hat{w}_{,\theta}. \end{aligned}$$

The boundary conditions may also be written in terms of the displacement rates as

$$\dot{v} = \dot{w} = \dot{w}_{,xx} = 0 \quad \text{at } x = 0 \quad (30)$$

and

$$\dot{u}_B = \dot{u}_S = \dot{v}_{,x} = \dot{w}_{,x} = 0 \quad \text{at } x = L/R. \quad (31)$$

The strain displacement relationships may be combined with the equilibrium and constitutive relationships to obtain a solution to the problem. However, the constitutive relationships as given in equation (15) are in a general form and must be specialized for the shell problem. This is done in the subsequent analysis.

STRESS STRAIN RELATIONS

In engineering practices, the property of a material is characterized by the nominal stress vs. nominal strains (S_{nom} vs. e) curve obtained from a uniaxial tensile test. Assuming the condition of conservation of mass, it may be shown that the uniaxial Kirchhoff stress, S , may be written as

$$S = \frac{S_{\text{nom}}}{1+e}. \quad (32)$$

Furthermore, the uniaxial Green strain, ε , may be expressed by

$$\varepsilon = e \left(1 + \frac{e}{2} \right). \quad (33)$$

Thus, with the two previous equations the nominal stress-strain curve can be converted into the Kirchhoff stress vs. Green strain curve.

The magnitude of the maximum elastic strain of a shell structure is usually small. Therefore, for an isotropic and homogeneous material, the elastic stress-strain relationship may be reasonably expressed by,

$$\dot{\epsilon}_{ij}^e = \frac{1}{E} [(1 + \nu)\dot{S}_{ij} - \nu\dot{S}_{kk}\delta_{ij}] \tag{34}$$

where E and ν are respectively Young’s modulus and Poisson’s ratio. The plastic stress-strain relationship depends on the loading function F and the proportionality function G , which strictly speaking, should be experimentally determined. Available experimental results indicate that the Mises’ yield function or loading function [17] leads to a good prediction of the initial yielding of an isotropic material. Furthermore, in the absence of Bauschinger effect and in a case of relatively small strain, the Mises’ function gives also a good prediction of the subsequent yielding. Usually, the Mises’ function or the second invariant of the deviatoric stress tensor has been expressed in terms of the true stress. For a case of small strain (although the rotation may be large), the difference between the value of the second invariant of the true stress tensor and that of the Kirchhoff stress tensor is relatively small. For the shell problem, it is expected that the foregoing conditions prevail. Therefore, it is assumed that

$$f = J_2 = \frac{1}{2}S'_{ij}S'_{ij} \tag{35}$$

where

$$S'_{ij} = S_{ij} - \frac{1}{3}\delta_{ij}S_{kk} \tag{36}$$

Employing the concept of isotropic hardening and assuming that the scalar function G is a function of the invariant J_2 only, G may be determined from the results of a simple tension test. It may be shown that

$$G = \frac{3}{4J_2} \left[\frac{1}{E_t} - \frac{1}{E} \right] \quad \text{for } J_2 > 0$$

$$G = 0 \quad \text{for } J_2 \leq 0 \tag{37}$$

where E_t is the tangent modulus obtained from the uniaxial Kirchhoff stress vs. Green strain curve. Furthermore, the conditions $J_2 > 0$, $J_2 = 0$ and $J_2 < 0$ specify respectively the conditions of loading, neutral loading and unloading.

Turning now to expressing explicitly the stress rates in terms of strain rates for the shell, the assumption of plane stress and the relations given by equations (12), (34)–(37) are employed. Carrying out the relevant substitutions, the Kirchhoff stress rates may be expressed as

$$\begin{aligned} \dot{S}_1 = \dot{S}_x &= f_{11}\dot{\epsilon}_x + f_{12}\dot{\epsilon}_\theta + f_{13}\dot{\gamma}_{x\theta} \\ \dot{S}_2 = \dot{S}_\theta &= f_{12}\dot{\epsilon}_x + f_{22}\dot{\epsilon}_\theta + f_{23}\dot{\gamma}_{x\theta} \\ \dot{S}_3 = \dot{S}_{x\theta} &= f_{13}\dot{\epsilon}_x + f_{23}\dot{\epsilon}_\theta + f_{33}\dot{\gamma}_{x\theta} \end{aligned} \tag{38}$$

where the symmetric matrix of coefficients f_{ij} may be expressed in terms of the inverse of the matrix c_{ij} as

$$f_{ij} = c_{ij}^{-1} \quad i, j = 1, 2, 3 \tag{39}$$

where

$$\begin{aligned}
 c_{11} &= \frac{1}{E} + \frac{G}{9}(2S_x - S_\theta)^2 \\
 c_{12} &= \frac{-\nu}{E} + \frac{G}{9}(2S_x - S_\theta)(2S_\theta - S_x) \\
 c_{13} &= \frac{G}{3}(2S_x - S_\theta)2S_{x\theta} \\
 c_{22} &= \frac{1}{E} + \frac{G}{9}(2S_\theta - S_x)^2 \\
 G_{23} &= \frac{G}{3}(2S_\theta - S_x)(2S_{x\theta}) \\
 c_{33} &= \frac{2(1+\nu)}{E} + G(2S_{x\theta})^2.
 \end{aligned} \tag{40}$$

The value of G is defined as in equation (37) with

$$J_2 = \frac{1}{3}(S_x^2 - S_\theta S_x + S_\theta^2) + S_{x\theta}^2. \tag{41}$$

It should be noted that this form of the invariant differs from the form used by many previous solutions (1)–(5) utilizing the bifurcation approach in that the present state of S_θ and $S_{x\theta}$ are considered important as well as the axial stress S_x , if prebuckling deformations are to be considered.

For a general work hardening material, a numerical description of the Kirchhoff stress vs. Green strain curve is needed for the numerical computation. In the subsequent numerical solution, the stress–strain curve is approximated by choosing P_e points on the curve in addition to the origin. Furthermore, the segment of the curve from the origin to the first point is considered linear with subsequent curve segments approximated by piecewise parabolic sections with continuous slopes at each point.

METHOD OF SOLUTION

The functional I involved in the variational principle expressed by equation (16) may now be specialized to the case of axially compressed cylindrical shells in the form

$$\begin{aligned}
 I = R^3 \int_0^{L/R} \int_0^{2\pi/m_0} \int_{-h/2R}^{h/2R} & (\dot{S}_x \dot{\epsilon}_x + \dot{S}_\theta \dot{\epsilon}_\theta + \dot{S}_{x\theta} \dot{\gamma}_x + S_x \dot{w}_{,x}^2 + S_\theta \dot{w}_{,\theta}^2 \\
 & + 2S_{x\theta} \dot{w}_{,x} \dot{w}_{,\theta}) dz d\theta dx - 2\dot{P}R^2 \int_0^{2\pi/m_0} \dot{u}(0, \theta) d\theta
 \end{aligned} \tag{42}$$

where \dot{P} is the applied axial traction rate and m_0 is an integer multiple of the number of periodic circumferential waves. Employing equation (38), the functional I may be written

as

$$\begin{aligned}
 I = R^3 \int_0^{L/R} \int_0^{2\pi/m_0} \int_{-h/2R}^{h/2R} \{ & f_{11}\dot{\epsilon}_x^2 + f_{22}\dot{\epsilon}_\theta^2 + f_{33}\dot{\gamma}_{x\theta}^2 + 2f_{12}\dot{\epsilon}_\theta\dot{\epsilon}_x \\
 & + 2f_{13}\dot{\epsilon}_x\dot{\gamma}_{x\theta} + 2f_{23}\dot{\epsilon}_\theta\dot{\gamma}_{x\theta} + S_x\dot{w}_{,x}^2 + S_\theta\dot{w}_{,\theta}^2 + 2S_{x\theta}\dot{w}_{,x}\dot{w}_{,\theta} \} dz d\theta dx \\
 & - 2\dot{P}R^2 \int_0^{2\pi/m_0} \dot{u}(0, \theta) d\theta.
 \end{aligned} \tag{43}$$

A solution of the problem may be obtained by using the Rayleigh–Ritz method of variational calculus and a numerical procedure. Furthermore, since the loads are applied quasistatically, inertia forces may be neglected and an arbitrary time scale may be chosen such that the velocities and displacement increments have the same values. In other words rates and increments may be treated synonymously.

The following computational scheme is employed. The present state of stress, deformation and the condition of loading or unloading are assumed known at each point in the body. The velocity field may be represented by a number of chosen admissible functions with arbitrary coefficients. When these functions are substituted into the functional I , the latter becomes a function of the coefficients which may be chosen so that I has an extremum. After the velocity field is determined, the deformation, stress and material states of the body at a small time interval later may be determined. Subsequently, the condition of loading or unloading may be determined from the strain rates. If the assumed condition does not agree with the outcome, then the condition indicated by the outcome is assumed and the computation is repeated until the calculated and assumed loading or unloading conditions agree. Once a correct velocity field has been determined, the variational principle may be reapplied. By repeating this procedure the deformation process is obtained.

The coordinate functions are chosen such that each one independently satisfies the boundary conditions, equations (30) and (31). Furthermore, they may describe closely the deformation patterns associated with existing elastic solutions such as in Ref. [22]. The displacement rates are represented by

$$\begin{aligned}
 \dot{w} &= b_1g_1 + b_2g_2 + b_3g_3 \\
 \dot{v} &= b_4g_4 \\
 \dot{u}_s &= b_5g_5 + b_6g_6 + b_7g_7 + b_8g_8
 \end{aligned} \tag{44}$$

where $b_i (i = 1, \dots, 8)$ are arbitrary coefficients and the coordinate functions g_i are defined by

$$\begin{aligned}
 g_j &= e^{-\lambda_j x}(\cos 2\alpha_j x + \Gamma_j \sin 2\alpha_j x) - 1 \quad j = 1, 2 \\
 g_3 &= \sin \alpha x \sin \beta \theta \\
 g_4 &= \sin \alpha x \cos \beta \theta \\
 g_5 &= (L/R - x) \\
 g_{j+5} &= e^{-\lambda_j x}(\Delta_j \cos 2\alpha_j x + \Omega_j \sin 2\alpha_j x) - (x - L/R) - D_j \quad j = 1, 2 \\
 g_8 &= \cos \alpha x \sin \beta \theta
 \end{aligned} \tag{45}$$

with

$$\begin{aligned}
 \Gamma_j &= \frac{\lambda_j^2 - 4\alpha_j^2}{4\alpha_j\lambda_j} & j = 1, 2 \\
 \alpha &= \frac{2n+1}{2} \frac{\pi}{L/R} & n = 1, 2, \dots \\
 \beta &= m m_0 & m = 1, 2, \dots \\
 \Delta_j &= \frac{4\alpha_j^2 - 3\lambda_j^2}{2\lambda_j(\lambda_j^2 + 4\alpha_j^2)} & j = 1, 2 \\
 \Omega_j &= \frac{12\alpha_j^2 - \lambda_j^2}{4\alpha_j(\lambda_j^2 + 4\alpha_j^2)} & j = 1, 2 \\
 D_j &= e^{-\lambda_j L/R} (\Delta_j \cos 2\alpha_j L/R + \Omega_j \sin 2\alpha_j L/R).
 \end{aligned}
 \tag{46}$$

The values of α and β are determined by the variational procedure, whereas the parameters $\alpha_j (j = 1, 2)$ are determined from the condition $\dot{w}_{,x} = 0$ at $X = L/R$ by the equation

$$\frac{\cos 2\alpha_j L/R}{2\lambda_j} + \frac{\sin 2\alpha_j L/R}{4\alpha_j} = 0 \quad j = 1, 2
 \tag{47}$$

which is solved for the value of α_j closest to the value of α . The values of λ_1 and λ_2 are chosen initially based on the elastic solution, and are adjusted for subsequent load increments depending upon the relative amplitudes of the respective coefficients.

The initial imperfection field was chosen to be of the form

$$\hat{w} = c_f \sin \alpha' x \sin \beta' \theta$$

where C_f , α' and β' are the constant amplitude and wave length to be chosen at the outset of the computation.

By combining equation (44) and equations (45) and (46) and substituting the results into equation (29) the functional I may be written in the form.

$$I = \sum_{j=1}^8 \sum_{j=1}^8 b_j b_i I_{ij} + \dot{P} \sum_{i=1}^8 I_{pi} b_i
 \tag{48}$$

where I_{ij} , symmetric with respect to i and j , is a definite integral of the form

$$I_{ij} = R^3 \int_0^{L/R} \int_0^{2\pi/m_0} \int_{-h/2R}^{h/2R} \bar{I}_{ij} dz d\theta dx.
 \tag{49}$$

The values of \bar{I}_{ij} are determined from the indicated substitutions and are seen to be functions of material property coefficients as well as the present state of stress and deformation. The values of I_{pi} are similarly determined by the indicated substitutions in the second term of equation (43).

In equation (48) the coefficients b_i are determined from the condition that the functional I has an extremum, i.e.

$$\frac{\partial I}{\partial b_i} = 2 \sum_{j=1}^8 b_j I_{ij} + \dot{P} I_{pi} = 0 \quad (i = 1, \dots, 8).
 \tag{50}$$

For a given loading rate \dot{P} and known values of I_{ij} and I_{pi} , the previous system of equations may be solved for the values b_i . However, when P reaches a maximum, \dot{P} will be zero and the solution of equation (50) may not be unique. To circumvent this difficulty, the average axial velocity under the applied load, \dot{u}_{av} , which is a monotonic function, is used as an additional constraint. \dot{u}_{av} is defined as

$$\dot{u}_{av} = \frac{m_0}{2\pi} \int_0^{2\pi/m_0} \left(\sum_{i=1}^3 \int_0^{L/R} b_i H_x g_{i,x} dx + \sum_{i=5}^8 b_i g_i \right) d\theta. \tag{51}$$

Instead of specifying the loading rate, the value of \dot{u}_{av} is assigned. Thus, equations (50) and (51) may be solved simultaneously for the corresponding nine unknowns, $b_i (i = 1, \dots, 8)$ and \dot{P} .

Knowing the present state of stress, deformation, λ_1 and λ_2 , and the desired average end displacement increment, the coefficients $b_i (i = 1, \dots, 8)$ and \dot{P} are determined for a particular value of the pair m and n , corresponding to the number of axial and circumferential waves respectively. The value of I may then be determined from equation (48). Next the value of I corresponding to $m + 1, n$ and $m, n + 1$ are calculated and the approximate value of $\partial I / \partial \alpha$ and $\partial I / \partial \beta$ are determined. The minimum value of I corresponding to, at most, a discrete increment of n or m may be determined by extrapolating from the derivatives $\partial I / \partial \alpha$ and $\partial I / \partial \beta$. Existing elastic solutions are helpful in determining an initial value for m and n . The procedure is believed sound since the deformation process will be continuous and a new value of α and β may be calculated for each prescribed end displacement increment.

Finally, the problem of numerically calculating the integrals in equation (43) is discussed. To alleviate the difficulty of keeping track of the material response of each point in the shell, the uniform shell is conceptually replaced by a structure composed of four thin load carrying cylindrical sheets, with a fixed spacing between any two sheets. Each sheet is made of a work hardening material. The z coordinate for each sheet is

$$z = \frac{h}{8R} (2q - 5) \quad q = 1, \dots, 4 \tag{52}$$

where q is defined as the sheet number. There is no stress variation through the thickness of each sheet which carries stress resultants equal to the products of the respective stress components and $h/4$. In addition each sheet is divided axially into $p_a - 1$ equal segments separated by p_a axial sections and then divided circumferentially, into $p_c - 1$ equal segments separated by p_c circumferential sections. The axial and circumferential coordinates given by the intersection of the axial and circumferential sections are

$$\begin{aligned} x &= \frac{r-1}{p_a-1} \frac{L}{R} & r &= 1, \dots, p_a \\ \theta &= \frac{s-1}{p_c-1} \frac{2}{m_0} & s &= 1, \dots, p_c. \end{aligned} \tag{53}$$

Consider the integral in equation (49) and let the following notation be introduced.

$$\bar{I}_{ij}(x, \theta, z) = \bar{I}_{ij}(r, s, q). \tag{54}$$

Thus the integration may be approximated by the following scheme:

$$\begin{aligned}
 R^3 \int_0^{L/R} \int_{-h/2R}^{h/2R} \int_0^{2\pi/m_0} \bar{I}_{ij} d\theta dx dz &= \frac{Rh\pi L}{2m_0(p_a-1)(p_c-1)} \sum_{q=1}^4 \\
 &\left\{ \sum_{r=2}^{p_a-1} \sum_{s=2}^{p_c-1} \bar{I}_{ij}(r, s, q) + \frac{1}{2} \sum_{r=2}^{p_a-1} (\bar{I}_{ij}(r, 1, q) + \bar{I}_{ij}(r, p_c, q)) \right. \\
 &\left. + \frac{1}{2} \sum_{s=2}^{p_c-1} (\bar{I}_{ij}(1, s, q) + \bar{I}_{ij}(p_a, s, q)) + \frac{1}{4} (\bar{I}_{ij}(1, 1, q) + \bar{I}_{ij}(1, p_c, q) + \bar{I}_{ij}(p_a, 1, q) + \bar{I}_{ij}(p_a, p_c, q)) \right\}. \tag{55}
 \end{aligned}$$

The foregoing numerical procedure has been incorporated into a computing program in Fortran language [23]. The results follow.

RESULTS AND DISCUSSION

Numerical results have been obtained by the foregoing procedure for four right circular cylinders, three of which buckled in the axisymmetric mode, and the fourth buckled in the non-symmetric or diamond shape mode. These four numerical results are believed to be representative of, and to agree favorably with the experimental results of Lee [3], as well as existing theories.

The experimental results of Lee were used for two reasons. First, the edges of the specimens were in a testing condition which would be considered quite close to that of a hinged edge. Secondly, the specimens were made of a relatively soft aluminum alloy, 3003-0, with nominal tensile stress-strain curve as given in Ref. [3], chosen because its properties are such as to magnify the differences between the critical buckling stresses of different geometries as well as that of different theories. The specimens used by Lee were of different lengths. However, the length of a specimen apparently had little effect on its buckling load; and for this reason all four cylinders investigated by the present procedure were assumed to be of the same length.

The four cylinders under investigation had the following geometric properties:

TABLE 1

Cylinder	R	2L	R/h	C _f	β'	α'
I	5.0	20.0	50.00	0.00	0.0	0.00
II	5.0	20.0	30.00	0.00	0.0	0.00
III	5.0	20.0	15.00	0.00	0.0	0.00
IV	5.0	20.0	46.06	0.01	4.0	3.92

with the numerical parameters $p_a = 50$, $p_c = 20$, $m_0 = 2$.

The theoretical deformation process of cylinders I-III are typified by that shown in Figs. 2 and 3. Figure 2 shows the variation in the average axial displacement with axial load, while Fig. 3 shows the calculated radial deflection profiles for various axial loads acting on cylinder I. Figure 3 indicates that the bending waves develop gradually at first and then grow rapidly as the maximum load is approached. The buckling process is characterized by an increasing rate of deformation, rather than an abrupt geometrical change implied by the idealized bifurcation approaches. It should be noted that cylinders I-III

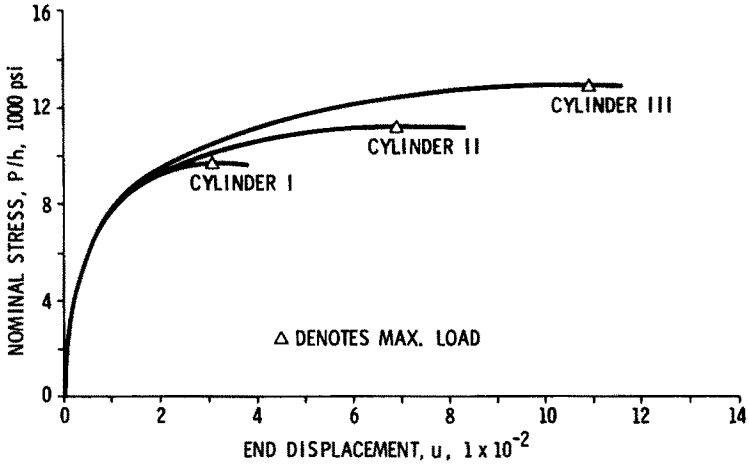


FIG. 2. Axial end displacement vs. applied axial load for cylinders I-III.

all exhibit unloading prior to reaching the maximum load as in [11], and similar to the phenomena observed in the inelastic buckling of columns [19, 20]. Also, the experimentally observed phenomena of successive failure and subsequent collapse of local bending waves near the hinged end is seen to occur.

For the range of R/h investigated, $15 < R/h < 50$, the results indicate that the axisymmetric mode of deformation is preferable for an initially perfect cylinder. However, if initial imperfections of sufficient amplitude are introduced, the present procedure may predict the diamond shape mode of deformation. A diamond pattern initial imperfection was introduced in cylinder IV, corresponding to Lee's [3] only sample which buckled in the diamond shape mode of deformation, and the present theory was applied. The radial coordinate function, corresponding to the diamond shape mode of deformation, increasingly became the most dominant component in the deformation process as the axial load approached the buckling load.

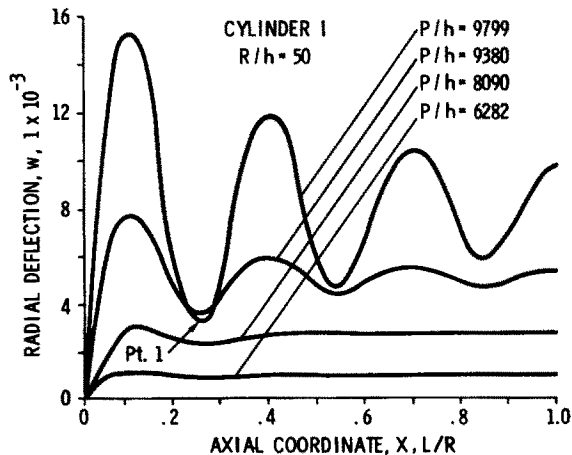


FIG. 3. Radial deflection profiles for cylinder I under various axial loads.

The initial buckling load predictions for different theories are presented in Fig. 4, along with the experimental results of Lee [3]. The upper and lower solid curves correspond to the critical bifurcation loads by the incremental [5] and deformation [2] theories, respectively, using the hinged end assumption. The middle solid curve corresponds to the same locus of critical loads as the upper solid curve except that the free edge assumption is used [7]. The present theory in which prebuckling deformation is considered, predicts maximum loads, hypothesized for axisymmetric deformation by the dashed curve which is seen to be considerably lower than the curve corresponding to the bifurcation approach by Batterman [5] using incremental theory and the hinged end assumption. For the range of parameters considered, the ordinary bifurcation approach using the free edge assumption predicts critical loads in quite good agreement with the present theory and experiment. A possible explanation may be that when using bifurcation analyses, prebuckling deformations are usually ignored, hence realistic boundary conditions may imply a buckling process which is not too realistic and the predicted critical load may be quite different from the actual maximum load. If on the other hand, unrealistic boundary conditions are assumed such that a more realistic buckling process is implied, a fairly accurate critical load may be predicted. Lee [9] has devised a more rigorous bifurcation approach, for the case of the axisymmetric deformation with edge constraints, in which the configuration just prior to buckling is approximated. A critical load of unloading is then calculated and is very close in value to the corresponding maximum loads by the present procedure. If deformation theory is considered, it is seen that buckling loads somewhat lower than experimental results may be predicted if prebuckling deformation and initial imperfections are considered. Finally, the numerical maximum load for cylinder IV and the corresponding experimental result for the diamond shape mode of deformation are presented on the same figure. Although for this case the comparison with experiment is not as favorable as in the axisymmetric case, it should be noted that the present procedure predicts a

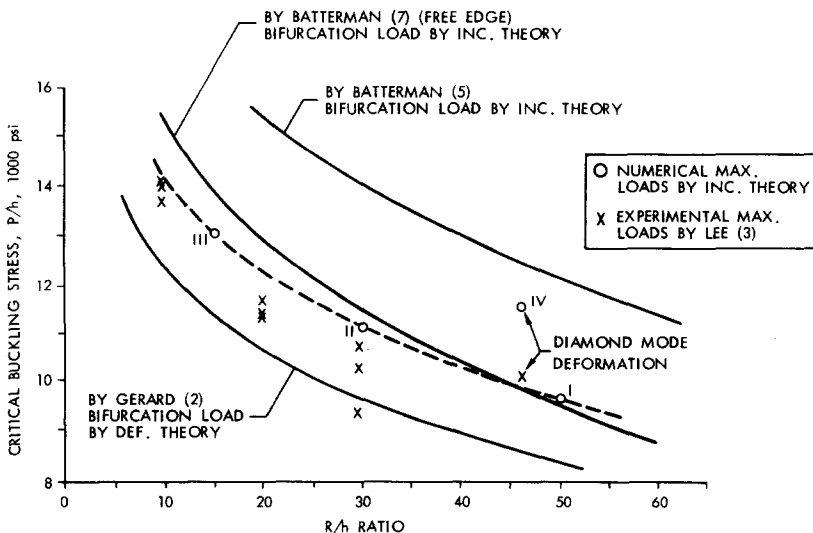


FIG. 4. Comparison of critical loads by different theories with experimental data.

maximum load which is substantially lower than the corresponding load by the idealized bifurcation approach using the incremental theory of plasticity.

CONCLUSIONS

The results of this investigation indicate that the variational principle developed in this paper for quasi-static problems of finite plasticity may be used to determine the deformation process of an inelastic body. By using the variational principle and the incremental Rayleigh–Ritz technique, the inelastic buckling process of axially compressed cylindrical shells with edge constraints can be reasonably predicted. It is found that the stress–strain relationship by the modified J_2 incremental theory, when employed concurrently with more realistic treatments of boundary conditions and pre-buckling finite deformation, yields a fairly accurate prediction of the buckling strength of a cylindrical shell.

Acknowledgments—This study was supported by the National Science Foundation under Grant GK-443 to the University of Notre Dame. The authors would also like to thank Mrs. Linda Mamaros and the Sandia Corporation for the preparation of this manuscript.

REFERENCES

- [1] P. P. BIJLAARD, Theory and tests on the plastic stability of plates and shells. *J. aeronaut. Sci.* **16**, 529–541 (1949).
- [2] G. GERARD, Compressive and Torsional Buckling of Thin-Wall Cylinders in Yield Region, NACA TN 3726 (1956).
- [3] L. H. N. LEE, Inelastic buckling of initially imperfect cylindrical shells subject to axial compression. *J. Aerospace Sci.* **29**, 87–95 (1962).
- [4] S. C. BATTERMAN and L. H. N. LEE, Effects of modes on plastic buckling of compressed cylindrical shells. *AIAA Jnl* **4**, 2255–2257 (1966).
- [5] S. D. BATTERMAN, Plastic buckling of axially compressed cylindrical shells. *AIAA Jnl* **3**, 316–325 (1965).
- [6] S. T. ARIARATNAM and R. N. DUBEY, Instability in an elastic plastic cylindrical shell under axial compression. *J. appl. Mech.* **36**, 47–50 (1969).
- [7] S. C. BATTERMAN, Free-edge plastic buckling of axially compressed cylindrical shells. *J. appl. Mech.* **35**, 73–79 (1968).
- [8] D. C. DRUCKER, A More Fundamental Approach to Plastic Stress–Strain Relations, *Proceedings of the First U.S. National Congress of Applied Mechanics*, pp. 487–491. ASME (1951).
- [9] G. H. HANDELMAN and W. H. WARNER, Loading paths and the incremental stress law. *J. math. Phys.* **33**, 157–164 (1954).
- [10] B. BUDIANSKY, A reassessment of deformation theories of plasticity. *J. appl. Mech.* **26**, 259–264 (1959).
- [11] L. H. N. LEE, Inelastic Behavior of Axially Compressed Cylindrical Shells Subject to Edge Constraints, *Developments in Mechanics*, Vol. 5, *Proceedings of 11th Midwestern Mechanics Conference*, Iowa State University, pp. 307–322 (1969).
- [12] J. L. SANDERS, H. G. MCCOMB and F. R. SCHLECHTE, A Variational Theorem for Creep with Application Plates and Columns, NACA, Rep. 1342 (1957).
- [13] R. S. ROTH, Plastic Buckling of Thin Shallow Spherical Shells, *Proceedings of the Fourth U.S. National Congress of Applied Mechanics*, pp. 1059–1065. ASME (1962).
- [14] R. HILL, A general theory of uniqueness and stability in elastic–plastic solids. *J. Mech. Phys. Solids* **6**, 236–249 (1958).
- [15] D. C. DRUCKER, Variational Principles in the Mathematical Theory of Plasticity, *Proc. Symposia in Appl. Math.*, Vol. VIII, *Calculus of Variations and Its Applications*, pp. 7–22. McGraw-Hill (1958).
- [16] Y. C. FUNG, *Foundations of Solid Mechanics*, pp. 127–153, 434–441. Prentice-Hall (1965).
- [17] P. M. NAGHDI, Stress–Strain Relations in Plasticity and Thermoelasticity, *Plasticity, Proc. 2nd Symposium on Naval Struct. Mech.*, p. 121. Pergamon Press (1960).
- [18] A. E. GREEN and P. M. NAGHDI, A General Theory of an Elastic–Plastic Continuum, Report No. AM-64-16, Division of Applied Mechanics, University of California, Berkeley, ONR Contract Nonr-222(69), Project NR064-436, 62 pp. (1964).

- [19] F. R. SHANLEY, Inelastic column theory. *J. aeronaut. Sci.* **14**, 261–267 (1947).
- [20] A. J. MALVICK and L. H. N. LEE, Buckling behavior of an inelastic column. *J. Engng Mech. Div. Am. Soc. civ. Engrs* **91**, 113–127 (1965).
- [21] L. H. N. LEE, Inelastic Buckling of Cylindrical Shells under Axial Compression and External Pressure, *Proceedings of the Fourth U.S. National Congress of Applied Mechanics*, pp. 989–998. ASME (1962).
- [22] W. FLUGGE, *Stresses in Shells*, pp. 210–212, 426–432, 457–463. Springer-Verlag (1960).
- [23] L. M. MURPHY, Effects of Edge Constraints and Large Deflections on the Inelastic Buckling of Cylindrical Shells under Axial Compression, Ph.D. Dissertation, University of Notre Dame (1968).
- [24] L. H. N. LEE and L. M. MURPHY, Inelastic Axisymmetric Buckling of Ring Stiffened Cylindrical Shells Under External Pressure, Report Number; Themis-UND-69-2, University of Notre Dame, Contract No. 014-68-A-0152 (NR 260-112/7-13-67) Office of Naval Research (1969).

(Received 29 January 1970; revised 17 November 1970)

Абстракт—В работе исследуются эффекты деформации до выпучивания, вызванные краевыми ограничениями и нелинейная зависимость деформаций на нелинейный процесс выпучивания осево сжатых цилиндрических оболочек. Пользуясь постулатом Дракера положительной работы в пластической деформации, выводится модифицированная теория пластичности мрщрцметмц для зависимости напряжение-деформация, представлена в терминологии Кирхгоффа и скорости деформации Грина. Дается вариационный принцип, в записи Лагранжа и для квази-статических задач конечной пластичности. Указывается принцип экстремума для материала, ооладающего достаточно большой скоростью упрочнения. Добавочно, определяется критерий для устойчивости тела под влиянием собственной нагрузки. Используется вариационный принцип вместе с способом приращения Релея-Ритца, для определения процесса деформации идеализированной цилиндрической оболочки, сложной из четырех тонких слоев, несущих нагрузку. Эти слоя изготовленные из материала об общем упрочнению. Теоретические предсказания, полученные численно на ВЦМ сравниваются удобно с доступными экспериментальными результатами.